

**A Numerical Estimation of the Effects  
of a cylindrical Hole and Imperfect Bonding  
on Stability of a Fiber in an Elastic Matrix**

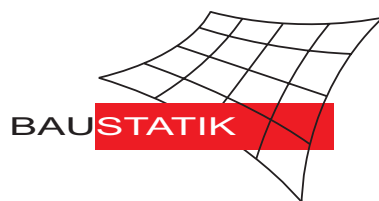
**Y. Lapusta, W. Wagner**

**Mitteilung 5(2001)**

**A Numerical Estimation of the Effects  
of a cylindrical Hole and Imperfect Bonding  
on Stability of a Fiber in an Elastic Matrix**

**Y. Lapusta, W. Wagner**

**Mitteilung 5(2001)**



# A NUMERICAL ESTIMATION OF THE EFFECTS OF A CYLINDRICAL HOLE AND IMPERFECT BONDING ON STABILITY OF A FIBER IN AN ELASTIC MATRIX

Yuri N. Lapusta <sup>a\*</sup> and Werner Wagner <sup>b</sup>

<sup>a</sup> *S. Timoshenko Institute of Mechanics, Nesterov Str. 3, Kiev, 03057, Ukraine*

<sup>b</sup> *Institut für Baustatik, Universität Karlsruhe (TH), Kaiserstr. 12, D-76131 Karlsruhe, Germany*

## Abstract

A simple numerical model based on three-dimensional analytical considerations is proposed for an estimation of the local effects of a cylindrical hole in the matrix as well as of fiber-matrix interface imperfections on compressive stability of fibers in fiber-reinforced composites. The geometry of the model includes an inclusion (a fiber) in a matrix with the assumption of an imperfect bonding at the interface and a cylindrical hole in the closest neighborhood. Then the problem formulation is idealized in two directions, providing a possibility of establishing lower and upper bounds for critical loads for the case of a matrix with a cylindrical hole of a non-circular cross-section as well as for the case of interface imperfections with the possibility of sliding without discontinuity of the displacements normal to the interface. The model takes into account the distinct difference in the properties of the fiber and the matrix and the spatial character of the problem at the microlevel. It is based on individual consideration of the fiber and the matrix with a hole with the necessity of satisfying certain idealized bonding conditions between them.

*Keywords: fibrous composites, stability, imperfect bonding, damage, bound estimation*

## 1 Introduction

It is commonly accepted that the compressive strength of fiber-reinforced composites can be limited by the possibility of occurring of fiber microbuckling in the matrix. Once this process begins, other degradation mechanisms can be triggered due to a subsequent redistribution of stresses.

---

\*Corresponding author. Address for correspondence in 1999-2002: Dr. Yuri Lapusta, Institut für Baustatik, Universität Karlsruhe (TH), Kaiserstr. 12, D-76131 Karlsruhe, Germany

Tel.: +49-(0)721-608-2283, Fax +49-(0)721-608-6015, E-mail: yuri.lapusta@bs.uni-karlsruhe.de

The possibility of fiber microbuckling in composite materials was first mentioned in [1]. The phenomenon was described as a longitudinal short-wave bending, similar to the case of a beam supported by an elastic foundation [2].

Numerous works were devoted since that time to experimental observations of the mentioned phenomenon as well as to developing analytical and computational models reflecting various aspects of the fiber microbuckling. The overwhelming majority of the models addressing the fiber-matrix buckling phenomena are two-dimensional and substitute in fact the 3D internal structure of fiber composites with a layered one. The first one seems to be proposed in [3], followed by many others, for example [4, 5, 6]. In [7] a question is posed on the applicability of the representation of fiber-reinforced composites by means of a layered medium. Many authors introduce in their models imperfections like initial fiber misalignment and waviness, in order to lower the predicted critical loads. Failure modes and various aspects connected with microbuckling and kinking-like phenomena were discussed among others in [8, 9, 10, 11, 12, 13].

Three-dimensional approaches to the problem of fiber microbuckling are less numerous because of substantially more complicated problem formulations. They are presented, among others, in [14, 15, 16, 17, 18, 19, 20]. In order to obtain solution of the problem, some authors use significant simplifications. For example, in [14], a three-dimensional description of the matrix behavior was combined with the beam theory for the description of the fibers. Reviews focusing on 3D approaches can be found in [18, 19]. Special attention in these reviews is given to the results based on the equations of the three-dimensional theory of stability of deformable bodies [21].

There also exist a great number of works addressing explicitly buckling of whole layers (isotropic or anisotropic) in laminated structures, with or without cracks and delaminations between them (see for example [18, 22, 23, 24, 25], which provide further references). This paper does not intend to review publications in this area, but we would like to mention principal distinctions of the present formulation in comparison to those works, dealing with buckling problems for layers in a composite. In the latter works the internal structure of unidirectional layers, which consists of fibers, matrices and fiber-matrix interfaces and is essentially three-dimensional, is smeared out by means of a homogenization procedure or by simply considering a sequence of uniform layers. Such approaches are sometimes called meso-approaches, because they correspond to the scale of interaction of layers in a layered structure. The questions posed by the present paper correspond to a quite different scale (the fiber-matrix scale and not to the layer-layer scale), with a qualitatively different geometry (3D and not 2D). This is the reason why these questions cannot be answered by means of some kind of a "layered" formulation with flat interfaces.

A review on the stability problems for laminated composites can be found in [18]. Some typical approaches and corresponding literature listings covering a broader spectrum of related problems for composite materials, including imperfections and interfacial effects, are presented in [26, 27, 28, 29, 30, 31, 32] and others. Failure theories for fibrous composites in compression are also reviewed in [5, 33].

It seems to be not possible to study such local effects as the effects of separate cylindrical holes in the matrix and of fiber-matrix interface imperfections on compressive stability in fiber-reinforced composites within the framework of substantially simplified approaches, like 1D or 2D ones, or continual theories. As a result, these phenomena and especially their combination were not sufficiently studied. Here, the aforementioned effects are estimated by means of developing a relatively simple 3D numerical model, which constitutes the novelty of this paper. The model is characterized by individual 3D consideration both of the fiber and the matrix weakened by a cylindrical hole. It proposes a procedure for determining three types of bounds for critical loading parameters, including lower and upper bounds for the case of a fiber in an elastic matrix near a cylindrical hole of a non-circular cross-section, bounds for the case of some bonding (adhesion) imperfections at the fiber-matrix interface without normal displacement discontinuity, as well as for a somewhat more general case in which both types of the defects are present. These bounds are based on numerical solutions of a model problem for a fiber near a cylindrical hole of a circular cross section in the matrix. The bonding conditions between the fiber and the matrix are satisfied numerically with a controlled accuracy in two cases, having an evident mechanical meaning. In the first case, all force and displacement components are continuous at the interfacial surface. In the second one, the shear force components both in the fiber and the matrix are equal to zero at the interface, while normal components of forces and displacements are continuous. The strategy proposed provides a possibility to consider the interface and the surface of the hole three-dimensionally and this way to avoid simplifications of the corresponding boundary conditions on these surfaces, inevitably imposed when using 1D, 2D, or continual approaches.

It is worth noting that this paper addresses three-dimensionally some important cases of micro-interactions at the fiber-matrix level, which are of interest nowadays due to the increasing need for improved micromechanics-based models. Neither the structural scale (i. e. the scale of the whole composite structure), nor the layer-layer scale (often called meso-scale), which are relatively more investigated, are not intended to be considered here. The main purpose of this paper is a consistent numerical estimation of the local effects which cannot be considered within the framework of meso- or macro-approaches. This includes phenomena occurring at the micro-scale (fiber-matrix scale) due to the mentioned above interactions between single fibers with a matrix and with a hole. The

formulation, which includes the mentioned above three types of bounds and incorporates not only effects of a hole, but also the possibility of imperfect bonding without normal displacement discontinuity, different instability modes, is based on and constitutes a substantial further development of previous research [17, 19, 20] in the direction concerned.

## 2 General assumptions and theoretical basis of the model

### 2.1 Geometry and bonding conditions. Some possible bounds for failure parameters.

The simplest 3D geometry enabling a prediction of the effects of holes and bonding imperfections on local compressive stability of fibers in composites subjected to compression should evidently include a long inclusion (a fiber) in a matrix and a cylindrical hole in the closest neighborhood. We refer the considered medium to Lagrangian coordinates  $x_i$  and make use as well of the local Lagrangian coordinates  $(r_q, \theta_q, z_q)$  ( $q = 1, 2$ ), which are associated with the fiber and the hole (Figs. 1, 2).

We assume that the inclusion (denoted henceforth by a superscript (1)) and the matrix (denoted further by a superscript (2)) consist in the general case of two distinctly different elastic isotropic materials with the mechanical constants  $E^{(1)}, \nu^{(1)}$ , and  $E^{(2)}, \nu^{(2)}$ , respectively. The matrix material is supposed to be substantially softer than that of the inclusion

$$E^{(1)}/E^{(2)} = \beta \gg 1. \quad (1)$$

Such a uniaxial compressive loading is considered that the shortenings of the fiber and matrix

along the axes  $z_q$  are equal

$$\varepsilon_{zz}^{0(1)} = \varepsilon_{zz}^{0(2)}. \quad (2)$$

We take into account the distinct difference in the properties of the fiber and the matrix and the spatial character of the problem at the local scale. To do this, it is necessary to consider individually the inclusion and the matrix with the necessity of satisfying some prescribed bonding conditions between them. The conditions between the fiber and the matrix can be satisfied exactly in the following two idealized cases, namely, when all force and displacement components are continuous

at the interfacial surface (this formulation corresponds to a perfect or ideal bonding and provides an upper bound for the case of an imperfect bonding at the interface) and when only normal components of forces and displacements are continuous while shear force components in the fiber and the matrix are equal to zero at the interface (considered as a lower bound). For the latter case, denoting the assumption of a sliding contact at the interface  $S_i$  without normal displacement discontinuity (without crack opening), the necessary contact conditions hold

$$t_{rz}^{(2)}|_{S_i} = t_{rz}^{(1)}|_{S_i} = t_{r\theta}^{(2)}|_{S_i} = t_{r\theta}^{(1)}|_{S_i} = 0, \quad t_{rr}^{(2)}|_{S_i} = t_{rr}^{(1)}|_{S_i}, \quad u_r^{(2)}|_{S_i} = u_r^{(1)}|_{S_i}, \quad (3)$$

where  $t_{ij}^{(q)}$  denote the components of the Kirchhoff stress tensor in the composite constituents.

For the perfect bonding the corresponding conditions hold

$$\begin{aligned} t_{rz}^{(2)}|_{S_i} = t_{rz}^{(1)}|_{S_i}, \quad t_{r\theta}^{(2)}|_{S_i} = t_{r\theta}^{(1)}|_{S_i}, \quad t_{rr}^{(2)}|_{S_i} = t_{rr}^{(1)}|_{S_i}, \quad u_z^{(2)}|_{S_i} = u_z^{(1)}|_{S_i}, \\ u_\theta^{(2)}|_{S_i} = u_\theta^{(1)}|_{S_i}, \quad u_r^{(2)}|_{S_i} = u_r^{(1)}|_{S_i}. \end{aligned} \quad (4)$$

The conditions of zero forces at the hole's internal surface  $S_h$  can be formulated as follows

$$N_i t_{ij}^{(2)}|_{S_h} = 0, \quad (5)$$

where  $N_i$  denote components of the normal unit to the surface  $S_h$  of the hole.

In case of a hole of a circular cross-section (Fig. 2), equations (5) give

$$t_{rz}^{(2)}|_{S_h} = t_{r\theta}^{(2)}|_{S_h} = t_{rr}^{(2)}|_{S_h} = 0. \quad (6)$$

Let  $p_{cr}^{sl}$  denote the critical value of the loading parameter  $p$  corresponding to condition (3) and  $p_{cr}^{id}$  to condition (4). Then, according to the physical sense, one should expect the following estimate for the critical loading parameter  $p_{cr}^{imp}$ , corresponding to the case of an interface with imperfections consisting in part of the areas with conditions of the type (3) and in part of the areas with conditions of the type (4)

$$p_{cr}^{sl} \leq p_{cr}^{imp} \leq p_{cr}^{id} \quad (7)$$

Relation (7) means that if, at some parts of the interface, the matrix supports the fiber only by means of stresses acting perpendicular to the surface and without the participation of the shear stresses, this would lead to a reduced support in comparison to the cases where all interface stresses participate.

A similar idealization of the problem formulation in two directions provides the following relatively simple possibility of establishing lower and upper bounds for critical loads for a matrix with a cylindrical hole of a noncircular cross-section (Fig. 1)

$$p_{cr}^{h1} \leq p_{cr}^h \leq p_{cr}^{h2}, \quad (8)$$

In (8)  $p_{cr}^h$  denote the critical value of a loading parameter corresponding to the problem for a fiber near a cylindrical hole of a non-circular cross section with the maximal dimension parameter of the cross-section equal to  $D_h < \infty$ ,  $p_{cr}^{h1}$  denote the critical value of the loading parameter corresponding to the case of a fiber near a cylindrical hole of a circular cross section of diameter equal to  $D_h$ , and  $p_{cr}^{h2}$  denote one of the two limiting cases  $\delta/D \rightarrow \infty$ ,  $D_h/D = const$  or  $D_h/D \rightarrow 0$ ,  $\delta/D = const$ .  $\delta$  denote the thickness of the spacing between the fiber-matrix interface and the surface of the hole, and  $D$  is fiber diameter. In simple words, relation (8) would mean that a "bigger" hole, as depicted schematically with dashed lines in Fig. 1, would weaken the supporting capability of the matrix and thus would reduce the critical compressive load, which seems to be in a good correspondence with the evident physical sense.

We further formulate and solve a model problem, which is used for the determination of  $p_{cr}^{sl}$ ,  $p_{cr}^{id}$  and  $p_{cr}^{h2}$ ,  $p_{cr}^{h1}$ .

## 2.2 Characteristic equation for the model problem

Consider a 3D instability problem for a fiber of diameter  $D$  near a cylindrical hole of a circular cross section of diameter  $D_h$  in an elastic matrix (Fig. 2). Assume that the fiber and the hole never intersect or touch each other, and their axes are parallel. The fiber lie in the region  $r_1 \leq D/2$ , and the hole in the region  $r_2 \leq D_h/2$ .

We suppose for simplicity  $\nu^{(1)} = \nu^{(2)} = \nu$ . This leads immediately to a homogeneous precritical states in the fiber and the matrix of the type



$$\begin{aligned}
\sigma_{zz}^{*0(1)} \neq 0, \quad \sigma_{zz}^{*0(2)} \neq 0, \quad \overline{\sigma_{zz}^{*0(1)}} \neq \overline{\sigma_{zz}^{*0(2)}}, \\
\sigma_{rr}^{*0(1)} = 0, \quad \sigma_{\theta\theta}^{*0(1)} = 0, \quad \sigma_{rr}^{*0(2)} = 0, \quad \sigma_{\theta\theta}^{*0(2)} = 0, \\
\varepsilon_{rr}^{0(1)} = \varepsilon_{\theta\theta}^{0(1)}, \quad \varepsilon_{rr}^{0(2)} = \varepsilon_{\theta\theta}^{0(2)}
\end{aligned} \tag{9}$$

After the linearization, the equilibrium equations in terms of displacement disturbances for a homogeneous medium hold [21]

$$\omega_{\alpha ij\beta} \frac{\partial^2 u_j}{\partial x_\alpha \partial x_\beta} = 0. \tag{10}$$

Coefficients  $\omega_{\alpha ij\beta}$  depend on the material properties and the precritical state. In the considered problem formulation, these equations should be independently applied to both the matrix and the inclusion.

Solutions of the equations (10) for precritical states like (9) can be represented [21] in the form

$$\begin{aligned}
u_r = \frac{1}{r} \frac{\partial \psi}{\partial \theta} - \frac{\partial^2 \chi}{\partial r \partial z}, \quad u_\theta = -\frac{\partial \psi}{\partial r} - \frac{1}{r} \frac{\partial^2 \chi}{\partial \theta \partial z}, \\
u_z = (\omega_{1133} + \omega_{1313})^{-1} (\omega_{1111} \Delta_1 + \omega_{3113} \frac{\partial^2}{\partial z^2}) \chi; \quad \Delta_1 = \frac{\partial^2}{\partial r^2} + \frac{1}{r} \frac{\partial}{\partial r} + \frac{1}{r^2} \frac{\partial^2}{\partial \theta^2};
\end{aligned} \tag{11}$$

with

$$\chi = \psi_2 + \psi_3, \quad (\Delta_1 + \zeta_j^2 \frac{\partial^2}{\partial z^2}) \psi_j = 0, \quad (j = 1, 2, 3). \tag{12}$$

Coefficients  $\zeta_j^2$  ( $j = 1, 2, 3$ ), which depend as well on the material parameters and the precritical state, must be determined in the following way

$$\zeta_1^2 = \omega_{3113} \omega_{1221}^{-1}, \quad \zeta_{2,3}^2 = c \pm (c^2 - \omega_{3333} \omega_{1111}^{-1} \omega_{3113} \omega_{1331}^{-1})^{1/2}, \tag{13}$$

$$2c \omega_{1111} \omega_{1331} = \omega_{1111} \omega_{3333} + \omega_{1331} \omega_{3113} - \omega_{3131} \omega_{1133} (\omega_{1313} + \omega_{3311}).$$

It is necessary to calculate the minimal value of the loading parameter for which equations (12), applied separately to the matrix and the inclusion, have nontrivial solutions  $\psi_j^{(q)}$ , ( $q = 1, 2$ ,  $j = 1, 2, 3$ ), describing a possible stability loss form of a fiber near a hole. These solutions should satisfy conditions (3) and (6), or (4) and (6), in dependence on the considered case, and attenuate while moving away from the fiber and the hole

$$u_r^{(2)} \rightarrow 0, \quad u_\theta^{(2)} \rightarrow 0, \quad u_z^{(2)} \rightarrow 0 \quad (r_1 \rightarrow \infty). \quad (14)$$

The geometry of the problem for a fiber near a circular cylindrical hole has a plane of symmetry, namely the plane containing the axes of the fiber and the hole. Therefore in this problem formulation one can, theoretically speaking, consider separately the following two types of possible stability loss forms (s.l.f.s): symmetric with respect to this plane ones, further referred as s.l.f.s of the first type, and s.l.f.s without any symmetry with respect to this plane, further referred as s.l.f.s of the second type.

Functions  $\psi_j^{(1)}$  for the fiber corresponding to the s.l.f.s of the first type can be represented as follows

$$\begin{aligned} \psi_1^{(1)} &= \gamma \sin \gamma z \sum_{n=1}^{\infty} A_{n,1}^{11} I_n(\zeta_1^{(1)} \gamma r_1) \sin n\theta_1, \\ \psi_s^{(1)} &= \cos \gamma z \sum_{n=0}^{\infty} A_{n,s}^{11} I_n(\zeta_s^{(1)} \gamma r_1) \cos n\theta_1, \quad \gamma = \pi l^{-1}, \quad s = 2, 3. \end{aligned} \quad (15)$$

Corresponding functions  $\psi_j^{(2)}$  for the matrix should have the form

$$\begin{aligned} \psi_1^{(2)} &= \gamma \sin \gamma z \sum_{q=1}^2 \sum_{n=1}^{\infty} A_{n,1}^{2q} K_n(\zeta_1^{(2)} \gamma r_q) \sin n\theta_q, \\ \psi_s^{(2)} &= \cos \gamma z \sum_{q=1}^2 \sum_{n=0}^{\infty} A_{n,s}^{2q} K_n(\zeta_s^{(2)} \gamma r_q) \cos n\theta_q, \quad s = 2, 3. \end{aligned} \quad (16)$$

Solutions for the s.l.f.s of the second type are constructed similarly. In (15) and (16)  $l$  denote the length of the half-wave of the s.l.f.,  $I_n(x)$  and  $K_n(x)$  denote the modified Bessel functions and Macdonald functions, respectively.

Solutions for the matrix must then be represented in each of the coordinate systems  $(r_q, \theta_q, z_q)$  and satisfy, together with the solutions for the fiber, the conditions (3) and (6), or (4) and (6), depending on the considered case. After a change of variables

$$\begin{aligned} X_{n,j}^{11} &= A_{n,j}^{11} I_n(\zeta_j^{(1)} \gamma R), \quad X_{n,j}^{21} = A_{n,j}^{21} K_n(\zeta_j^{(2)} \gamma R), \\ X_{0,s-1}^{11} &= A_{0,s}^{11} I_0(\zeta_s^{(1)} \gamma R), \quad X_{0,s-1}^{21} = A_{0,s}^{21} K_0(\zeta_s^{(2)} \gamma R), \quad R = D/2, \end{aligned} \quad (17)$$

$$(n = 1, 2, \dots, \infty; j = 1, 2, 3; s = 2, 3),$$

and a similar change of the other unknown constants involved in the solutions, we obtain an infinite homogeneous system of algebraic equations in the matrix form

$$B_{\alpha k}^2 X_k^{21} + B_{\alpha k}^1 X_k^{11} + \sum_{n=0}^{\infty} Q_{\alpha kn} X_n^{22} = 0, \quad (18)$$

$$B_{vk}^2 X_k^{22} + \sum_{n=0}^{\infty} Q_{vkn} X_n^{21} = 0, \quad (\alpha = 1, 2; v = 3; k = 0, 1, 2, \dots, \infty).$$

In (18)  $X_n^{11}$ ,  $X_n^{2q}$  denote column vectors of the unknown constants.

The obtained infinite homogeneous systems of algebraic equations are then reduced to the canonical form

$$X_k^{21} + \sum_{n=0}^{\infty} M_{1kn} X_n^{22} = 0, \quad X_k^{22} + \sum_{n=0}^{\infty} M_{2kn} X_n^{21} = 0, \quad (19)$$

where

$$M_{1kn} = [B_{2k}^2 - B_{2k}^1 (B_{1k}^1)^{-1} B_{1k}^2]^{-1} [Q_{2kn} - B_{2k}^1 (B_{1k}^1)^{-1} Q_{1kn}], \quad (20)$$

$$M_{2kn} = (B_{3k}^2)^{-1} Q_{3kn}.$$

One derives subsequently characteristic equations in the form

$$\Delta^\mu(p, \kappa, \beta, \nu, \delta/D, D_h/D) = 0, \quad (21)$$

which include infinite determinants in their left-hand sides and must be numerically solved. In (21)  $\kappa$  and  $p$  denote the wave formation and loading parameters, respectively. They can be selected as follows

$$p = -\varepsilon_{zz}^{0(1)} = -\varepsilon_{zz}^{0(2)}, \quad \kappa = \kappa^{(1)} = \kappa^{(2)} = \pi D / (2l) \quad (22)$$

In (21) value  $\mu = 1$  corresponds to s.l.f.s of the first type, while  $\mu = 2$  to s.l.f.s of the second type.

### 3 Numerical results

#### 3.1 On the numerical procedure and its convergence

We have to calculate functions  $p_i = p_i(\kappa)$  for fixed values of the initial parameters of the problem and then minimize the obtained results to determine critical loads. Therefore, the critical value of  $p$ , corresponding to the critical stability loss form of a fiber near a hole for given values of  $\beta = E^{(1)}/E^{(2)}$ ,  $\nu$ ,  $D_h/D$  and  $\delta/D$ , is determined according to the following equations

$$p_{mi} = \min_{\kappa \neq 0} p_i(\kappa), \quad p_{cr} = \min_i (p_{mi}) \quad (23)$$

In the numerical solution of the problem we replace the infinite determinants by determinants of a certain finite size. This can be substantiated by the fact that the obtained infinite determinants are of the normal type.

To prove this we use the equivalence relationships in the form

$$I_n(x) \sim \frac{1}{n!} \left(\frac{x}{2}\right)^n, \quad K_n(x) \sim \frac{(n-1)!}{2} \left(\frac{x}{2}\right)^{-n}, \quad n \rightarrow \infty \quad (24)$$

and consider a series composed of expressions of the type

$$C_1 k^\eta \frac{(n+k-1)! (\zeta_j^{(2)})^k (\gamma D/2)^k (\zeta_j^{(2)})^n (\gamma D_h/2)^n}{(n-1)! k! (\zeta_j^{(2)})^{k+n} (2\delta + D + D_h)^{k+n}} \quad (25)$$

This series can be used as a majorizing series for the series

$$\sum_{k=0}^{\infty} \sum_{n=0}^{\infty} \sum_{i=1}^3 \sum_{j=1}^3 |M_{qkn,ij}|, \quad (q = 1, 2), \quad (26)$$

where  $M_{qkn,ij}$  denote elements of the matrix appearing in the canonical form (19), (20) of the obtained infinite systems of algebraic equations,  $C_k$  denote sufficiently large positive constants, and  $\eta$  is a natural number.

The value of (25) is less than

$$C_2 k^\eta \left(\frac{D}{D+\delta}\right)^k \left(\frac{D_h}{D_h+\delta}\right)^n \quad (27)$$

Series composed of expressions of the type (27) converge by virtue of the D'Alembert limit criterion. The latter implies that the aforementioned numerical procedure must converge.

Table 1 demonstrates the practical convergence of the numerical procedure employed. In this Table, a comparison of the values of  $p_{cr}^{id}$ , calculated with  $\nu = 0.3$ ;  $\beta = 200$ ;  $D_h/D = 1, 2, 4$ ,  $\delta/D = 0.15, 0.50$  and different dimensions  $N$  of the truncated determinant of the system (18), is presented. Here and henceforth, the superscript or abbreviation *id* denotes the correspondence of the calculated solutions to the conditions (4), while the superscript *sl* will denote the case (3). Table 2 presents results on the practical convergence of the numerical procedure while calculating the values of  $p_{cr}^{sl}$ . The convergence is even better, as  $\delta/D$  increase and  $D_h/D$  decrease. The results provided demonstrate a good practical convergence of the procedure proposed.

### 3.2 A numerical estimation of the effects of a hole

In order to estimate numerically the effects of a cylindrical hole of non-circular cross-section on stability of a fiber in a matrix we calculate the values  $p_{cr}^{h1}$  and  $p_{cr}^{h2}$  and use them as a lower and an upper bounds according to (8). The calculations are carried out for  $\beta = 200$  and  $\nu = 0.3$ . Fig. 3 presents solutions of the characteristic equation in the form of dependencies of the loading parameter  $p^{id}$  on the wave formation parameter  $\kappa$ , calculated for the s.l.f.s of the first type with  $D_h/D = 4$  and different values of  $\delta/D$ . Calculated curves for the s.l.f.s of the second type, which looked similar to the displayed curves, but corresponded to somewhat higher loading levels, were not depicted in Fig. 3, in order to keep the Figure understandable. Each point on the curves presented correspond to a certain instability mode with a half-wave  $l = \pi D/(2\kappa)$ . The minima of the curves can be considered as the critical parameters  $p_{cr}^{id}$  leading to the stability loss with a half-wave  $l_{cr} = \pi D/(2\kappa_{cr})$ .

A comparison of the values of  $p_{mi}^{id}$  corresponding to minima of the functions  $p^{id} = p^{id}(\kappa)$  calculated in the presence of a perfect bonding between the fiber and the matrix with allowance for the effects of a hole of a diameter  $D_h = 4D$  for the cases of a s.l.f. of the fiber of the first type (denoted as values  $p_{m1}^{id}$ ) and of the second type (values  $p_{m2}^{id}$ ) is given in Fig. 4. This comparison shows that the s.l.f. of the fiber of the first type is more likely to occur because it corresponds to smaller loads. Values  $p_{m1}^{id}$  can therefore be considered as critical for the case of a perfect bonding between the fiber and the matrix.

The critical values of the loading parameter  $p_{cr}^{id}$ , calculated in dependence on the dimensionless diameter of the cylindrical hole  $D_h/D$  for the dimensionless spacing between the fiber and the hole  $\delta/D$  equal to 0.15, 0.50, 1.00, 1.50 for the case of a perfect fiber-matrix bonding are plotted in Fig. 5. According to inequalities (8), these calculated values can be used as lower bounds  $p_{cr}^{h1,id}$  for critical loads for a matrix with a cylindrical hole of a noncircular cross-section (Fig. 1), in the presence of a perfect fiber-matrix bonding. The dashed curve in Fig. 5 denotes the corresponding upper bound  $p_{cr}^{h2,id}$  for critical loads, again according to (8). At the same time, the results presented in Fig. 5 constitute upper bounds  $p_{cr}^{id}$  for the estimate (7).

Similar results for a fiber near a cylindrical hole, but this time corresponding to the case of a sliding contact between the fiber and the matrix (values  $p_{cr}^{sl}$ ), calculated in dependence on the dimensionless diameter of the hole  $D_h/D$  for different values of the dimensionless spacing between the fiber and the hole ( $\delta/D = 0.15, 0.50, 1.00, 1.50$ ) are given in Fig. 6. With account of (8), these results can be used as lower bounds  $p_{cr}^{h1,sl}$  for critical loads for a fiber in a matrix with a cylindrical

hole of a noncircular cross-section (Fig. 1) in the presence of a sliding contact between the fiber and the matrix. Again, the dashed curve in Fig. 6 denotes the corresponding upper bound  $p_{cr}^{h2,sl}$  for critical loads, according to (8). On the other hand, the numerical results presented in Fig. 6 constitute lower bounds  $p_{cr}^{sl}$  employed in the estimate (7).

Following results concern a quantitative estimation of the possible effects of a hole on the critical values of the loading parameter by means of calculating the coefficient  $C_{ho} = (p_{cr}^{h2}/p_{cr}^{h1} - 1)$ . This coefficient denotes to what extent the calculated values of  $p_{cr}^{h2}$  can be higher than  $p_{cr}^{h1}$ . The effects of a cylindrical hole of a noncircular cross-section (Fig. 1), depending on its geometrical parameters, can lead to some intermediate value between 0 and  $C_{ho}$ , approaching in the most unfavorable cases the maximal value of  $C_{ho}$ . Fig. 7 presents the values of the parameter  $C_{ho}^{id}$  versus the dimensionless diameter of the hole  $D_h/D$  calculated for the case of an ideal fiber-matrix bonding with  $\delta/D = 0.15, 0.5, 1.0, 1.5$ . Similar results for  $C_{ho}^{sl}$  for the case of a sliding contact between the fiber and the matrix are given in Fig. 8.

### 3.3 A numerical estimation of the effects of adhesion imperfections

In order to estimate the effects of adhesion imperfections one has to calculate the values  $p_{cr}^{sl}$  and compare them with the corresponding values  $p_{cr}^{id}$  for the same prescribed set of geometrical and mechanical parameters of the problem. The mentioned values can then be used as a lower and an upper bound for the case of an interface with bonding imperfections according to (7). Solutions of characteristic equations (21) in form of calculated dependencies of the loading parameter  $p$  ( $p^{id}$  and  $p^{sl}$ ) on the wave formation parameter  $\kappa$  with  $\nu = 0.3$ ,  $\beta = 200$  and  $\delta/D = 0.15, 1.5$ , in the presence of a perfect bonding and a sliding contact between the fiber and the matrix, are presented in Fig. 9. The depicted dependencies correspond to the cases of a s.l.f. of the fiber of the first type, which provided smaller values of  $p$ .

For the case of a sliding contact between the fiber and the matrix, we present (Fig. 10) results of a comparison of the values of  $p_{mi}^{sl}$ , corresponding to minima of the functions  $p_i^{sl} = p_i^{sl}(\kappa)$ , calculated for the s.l.f.s of the fiber in the matrix of the first type (values  $p_{m1}^{sl}$ ) and of the second type (values  $p_{m2}^{sl}$ ), with allowance for the effects of a hole of a diameter  $D_h = 4D$ . This comparison shows that, in the presence of a sliding contact too, the s.l.f.s of the fiber of the first type correspond to smaller loads, and the values  $p_{m1}^{sl}$  depicted in Fig. 10 can be considered as critical for the case considered, i. e.  $p_{cr}^{sl} = p_{m1}^{sl}$ .

In order to quantitatively evaluate the possible influence of bonding imperfections we calculate the

coefficient  $C_{ad} = (p_{cr}^{id}/p_{cr}^{sl} - 1)$  denoting to what extent the calculated values of  $p_{cr}^{id}$  can be higher than  $p_{cr}^{sl}$ . The effects of bonding imperfections can lead to some intermediate value between 0 and  $C_{ad}$ , approaching in the most unfavorable cases the maximal value of  $C_{ad}$ . Fig. 11 presents the values of the parameter  $C_{ad}$  versus the dimensionless diameter of the cylindrical hole  $D_h/D$  calculated with different values of the dimensionless spacing between the fiber and the hole  $\delta/D$ . Fig. 12 plots as well functions  $C_{ad} = C_{ad}(\kappa)$ , where  $C_{ad} = (p_{cr}^{id}(\kappa)/p_{cr}^{sl}(\kappa) - 1)$  calculated for  $\delta/D = 0.15, 0.5, 1.5, \rightarrow \infty$ .

### 3.4 On the joint effects of a hole and adhesion imperfections

One can estimate the range of the joint effects of a hole and adhesion imperfections on stability of a fiber in a matrix by means of comparing an 'ideal' case of a homogeneous matrix without holes in the presence of a perfect bonding at the fiber-matrix interface with a case of a matrix weakened by a hole in the presence of a sliding contact at the interface. The 'ideal' case correspond to one of the two limiting cases  $\delta/D \rightarrow \infty, D_h/D = const$  or  $D_h/D \rightarrow 0, \delta/D = const$ , which provide equal results within the framework of the discussed numerical model. Dependencies of the loading parameter  $p$  on the wave formation parameter  $\kappa$  for the aforementioned 'ideal' case (denoted as *id*,  $\delta/D \rightarrow \infty$ ) as well as for a fiber in a matrix with a hole in the presence of a sliding contact at the interface (denoted as *sl*, with  $\delta/D < \infty$ ) calculated with  $D_h/D = 4$  and different values of  $\delta/D$  are presented in Fig. 13. All depicted graphs correspond to the s.l.f.s of the first type, which had some advantage (corresponded to lower load levels) as compared with the s.l.f.s of the second type.

We introduce as a quantitative measure of mentioned above joint effects a parameter  $C_{ad+ho} = (p_{cr}^{h2,id}/p_{cr}^{h1,sl} - 1)$ . This coefficient indicates to what extent the calculated values of  $p_{cr}^{h2,id}$  for the 'ideal' case of a homogeneous matrix without defects can be higher than the value  $p_{cr}^{h1,sl}$ , corresponding to case of a fiber in a matrix with a hole, in the presence of a sliding contact at the interface. The effects of a cylindrical hole of a noncircular cross-section (like depicted in Fig. 1) combined with the influence of the bonding imperfections without normal displacement discontinuity at the very beginning of the stability loss, will depend on the shape of its cross-section and can lead to some intermediate value between 0 and  $C_{ad+ho}$ , approaching in the most unfavorable cases the maximal value of  $C_{ad+ho}$ . Fig. 14 presents these maximal values  $C_{ad+ho}$  in dependence on the dimensionless diameter of the hole  $D_h/D$ .

## 4 Conclusions

In this paper, a numerical model is developed for the quantitative estimation of the effects of a cylindrical hole and an imperfect fiber-matrix bonding on stability of a system fiber-matrix subjected to compression. The model presents a procedure for determining three types of bounds for critical loading parameters, including lower and upper bounds for the case of a fiber in an elastic matrix near a cylindrical hole of a non-circular cross-section, bounds for the case of some adhesion imperfections at the fiber-matrix interface without normal displacement discontinuity, as well as for a somewhat more general case in which both types of the defects are present. The model is based on individual consideration of the fiber and the matrix with the necessity of satisfying certain idealized bonding conditions between them. It takes this way into account the distinct difference in the properties of the fiber and the matrix and the spatial character of the problem at the microlevel. The bonding conditions between the fiber and the matrix are satisfied numerically with a controlled accuracy within the framework of the model discussed in two cases, namely, when all force and displacement components are continuous at the interfacial surface (this formulation is assumed to provide an upper bound for the case of an imperfect bonding at the interface) and when only normal components of forces and displacements are continuous while shear force components equal to zero at the interface both in the fiber and the matrix (considered as a lower bound for the cases without crack opening at the very beginning of stability loss). One of the simply realizable 3D models for a hole in the matrix, having a circular cross section with the axis parallel to the fiber axis, is employed in the paper for the estimation of the hole effects on the stability of situated nearby fibers with damaged and "ideal" fiber-matrix interface.

## Acknowledgements

This work has been supported in part by the Alexander von Humboldt-Stiftung and by the Deutsche Forschungsgemeinschaft through grant WA 746/12-1, which is gratefully appreciated.

## References

- [1] Dow NF, Grunfest IJ. Determination of most needed potentially possible improvements in materials for ballistic and space vehicles. *General Electric Co, Space Sci Lab* 1960; TISR 60 SD 389.



- [2] Timoshenko SP, Gere JM. *Theory of Elastic Stability*. Second Edition. New York, NY: McGraw-Hill Book Company, 1961.
- [3] Rosen BW. Mechanics of composite strengthening. *Fiber Composite Materials*, American Society of Metals, 1965; 37-75.
- [4] Schuerch H. Prediction of compressive strength in uniaxial boron fiber-metal matrix composite materials. *AIAA Journal* 1966; **4**(1):102-106.
- [5] Guynn EG, Bradley WL, Ochoa OO. A parametric study of variables that affect fiber microbuckling initiation in composite laminates: Part 1 - Analyses. *Journal of Composite Materials* 1992; **26**(11):1594-1616.
- [6] Chung I, Weitsman Y. On the buckling/kinking compressive failure of fibrous composites. *International journal of solids and structures* 1995; **32**(16):2329-2344.
- [7] Weitsman Y, Chung I. Can the compressive response of fiber-reinforced composites be modeled by means of layered arrays? *Journal of composite materials* 1996; **30**(6):662-671.
- [8] Evans AG, Adler WF. Kinking as a mode of structural degradation in carbon fiber composites. *Acta Metallurgica* 1978; **26**:725-738.
- [9] Budiansky B, Fleck NA. Compressive kinking of fiber composites: a topical review. *Applied Mechanics Reviews*, Part 2 1994; **47**(6):S246-S270.
- [10] Sun CT, Jun AW. Compressive strength of unidirectional fiber composites with matrix nonlinearity. *Composites science and technology* 1994; **52**(4):577-588.
- [11] Fleck NA, Shu JY. Microbuckle initiation in fibre composites: a finite element study. *Journal of the mechanics and physics of solids* 1995; **43**(12):1887-1918.
- [12] Soutis C, Turkmen D. Moisture and temperature effects of the compressive failure of CFRP unidirectional laminates. *Journal of Composite Materials* 1997; **31**(8):832-849.
- [13] Bazant ZP, Kim JH, Daniel IM, Becq-Giraudon E, Zi G. Size effect on compression strength of fiber composites failing by kink band propagation. *International journal of fracture* 1999; **95**(1):103-142.
- [14] Sadovsky MA, Pu SL, Hussain MA. Buckling of microfibers. *Journal of Applied Mechanics* 1967; December:1011-1016.
- [15] Guz AN. Construction of a theory of stability of unidirectional fiber composites. *Prikl Mekh* 1969; **5**(2):62-70 (in Russian).

- [16] Greszczuk LB. Microbuckling failure of circular fiber-reinforced composites. *AIAA Journal* 1975; **13**(10):1311-1318.
- [17] Lapusta YN. On the influence of the free surface of a cavity on fiber stability in an infinite matrix. *Proceedings of the XII Scientific Conference of Young Scientists of the Institute of Mechanics of the Ukrainian Academy of Sciences*, Kiev, Dept. in VINITI, July 1987; No.5389-87: 104-107 (in Russian).
- [18] Micromechanics of composite materials: Focus on Ukrainian research (edit. Guz AN). *Applied Mechanics Reviews*, Special Issue 1992; **45**(2):13-101.
- [19] Guz AN, Lapusta YN. Three-dimensional problems of the near-surface instability of fiber composites in compression (model of a piecewise-uniform medium) (Survey). *International Applied Mechanics* 1999; **35**(7):641-670.
- [20] Lapusta YN, Wagner W. On a role of fibre-matrix interfaces in the context of near-surface stability analysis of composite materials. *Proceedings of the Twelfth International Conference on Composite Materials (ICCM12)*, Paris, France, July 5th-9th 1999 (CD-ROM).
- [21] Guz AN. *Fundamentals of the Three-Dimensional Theory of Stability of Deformable Bodies*, Springer, 1999.
- [22] Biot MA. *Mechanics of Incremental Deformation*. First Edition. John Wiley & Sons: New York, 1965, 504 pp.
- [23] Guz IA. Estimation of critical loading parameters for composites with imperfect layer contact. *International Applied Mechanics* 1992; **28**:291-296.
- [24] Sprenger W, Gruttmann F, Wagner W. Delamination growth analysis in laminated structures with continuum based 3D-shell elements and a viscoplastic softening model. *Comp. Meth. in Appl. Mech. Engng.* 2000; **185**:123-139.
- [25] Remmers JJC, De Borst R, Riks E. Delamination buckling in fibre metal laminates. *Extended Abstracts of the Workshop on Recent Advances in Continuum Damage Mechanics for Composites*, 20-22 September 2000, ENS-Cachan, 15-16.
- [26] Zohdi T, Feucht M, Gross D, Wriggers P. A description of macroscopic damage through microstructural relaxation. *International Journal for Numerical Methods in Engineering* 1998; **43**(3):493-506.
- [27] Babich IYu, Semenyuk NP, Boriseiko AV. Stability and efficient design of cylindrical shells of metal composites subject to combination loading. *International Applied Mechanics* 1999; **35**(6):595-601.

- [28] Allix O, Ladevèze P, Gilletta D, Ohayon R. A damage prediction method for composite structures. *International Journal for Numerical Methods in Engineering* 1989; **27**(2):271-283.
- [29] Reifsnider KL. Modeling of the interphase in polymer-matrix composite material systems. *Composites* 1994; **25**(7):461-469.
- [30] Allix O, Ladevèze P, Vittecoq E. Modelling and identification of the mechanical behaviour of composite laminates in compression. *Composites science and technology* 1994; **51**(1):35-42.
- [31] Guz AN, Guz IA. On the theory of stability of laminated composites. *International Applied Mechanics* 1999; **35**(4):323-329.
- [32] Hutchinson JW, Suo Z. Mixed mode cracking in layered materials. *Advances in Applied Mechanics* 1991; **29**:63-191.
- [33] Schultheisz CR, Waas AM. Compressive failure of composites. *Prog. Aerospace Sci.* 1996; **32**:1-78.

Table 1: Practical convergence for  $p_{cr}^{id}$

	$D_h/D$	1	2		4
$\delta/D$	$N$			$N$	
0.15	24	0.0538	0.0507	42	0.0469
	33	0.0537	0.0500	51	0.0466
	42	0.0537	0.0499	60	0.0465
	51	0.0537	0.0499	69	0.0465
0.50	15	0.0571	0.0554	33	0.0500
	24	0.0556	0.0530	42	0.0495
	33	0.0555	0.0524	51	0.0493
	42	0.0555	0.0523	60	0.0492
	51	0.0555	0.0523	69	0.0492

Table 2: Practical convergence for  $p_{cr}^{sl}$

	$D_h/D$	1	2		4
$\delta/D$	$N$			$N$	
0.15	24	0.0452	0.0434	33	0.0412
	33	0.0447	0.0422	42	0.0402
	42	0.0447	0.0418	51	0.0397
	51	0.0447	0.0417	60	0.0394
	60	0.0447	0.0417	69	0.0393
0.50	15	0.0485	0.0474	33	0.0429
	24	0.0468	0.0451	42	0.0423
	33	0.0467	0.0444	51	0.0420
	42	0.0466	0.0442	60	0.0419
	51	0.0466	0.0441	69	0.0418

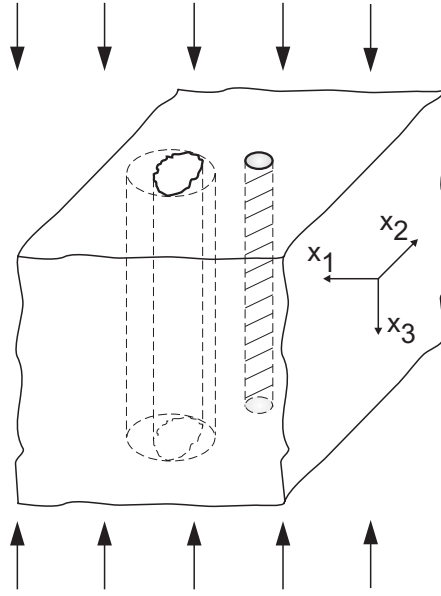


Figure 1: A long inclusion (a fiber) in a matrix and a hole in the closest neighborhood.

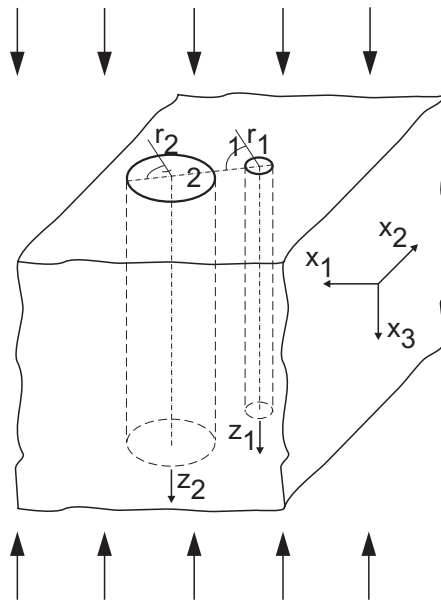


Figure 2: A model problem for a fiber near a cylindrical hole of a circular cross-section.

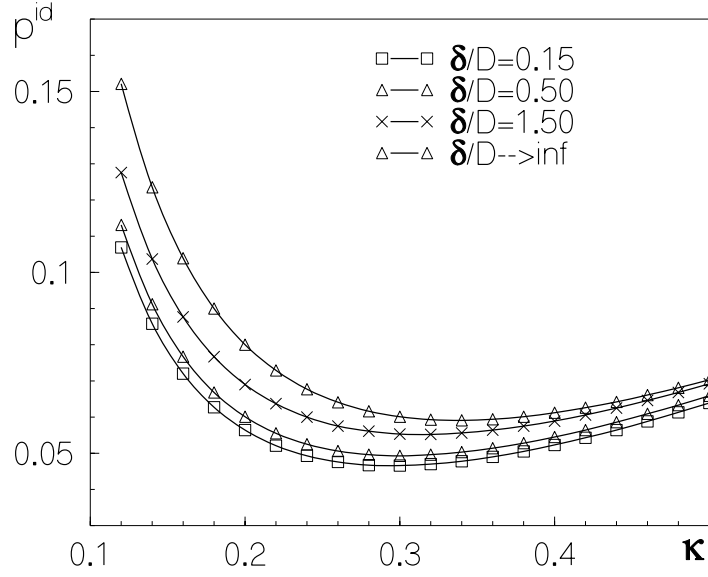


Figure 3: Dependencies of the parameter  $p^{id}$  on the wave formation parameter  $\kappa$ .

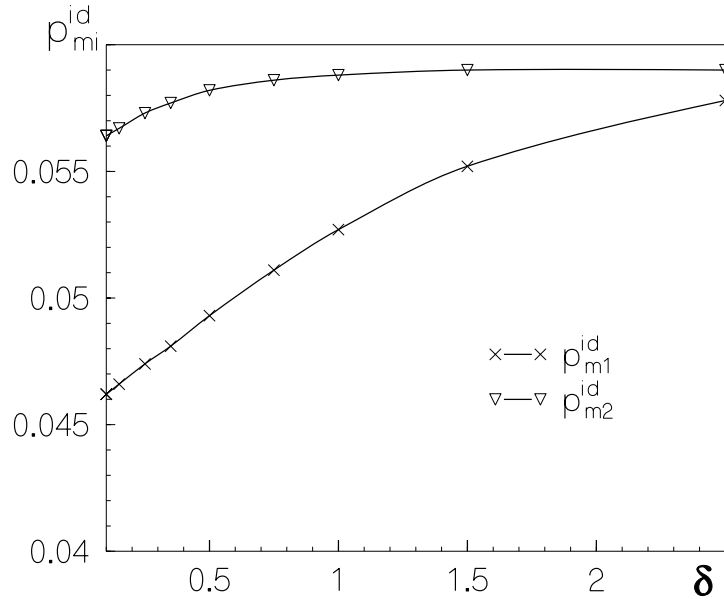


Figure 4: Values of  $p_{mi}^{id}$  calculated in the presence of a perfect bonding between the fiber and the matrix with allowance for the effects of a hole of a diameter  $D_h = 4D$  for the cases of a s.l.f. of the fiber of the first type (denoted as values  $p_{m1}^{id}$ ) and of the second type (values  $p_{m2}^{id}$ ).

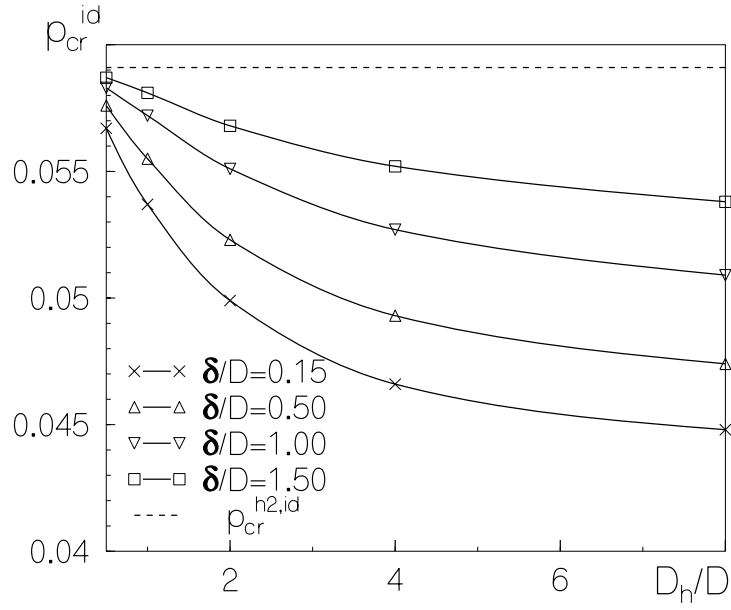


Figure 5: Parameter  $p_{cr}^{id}$  versus  $D_h/D$  for different values of the dimensionless spacing between the fiber and the hole  $\delta/D$  (the case of a perfect fiber-matrix bonding).

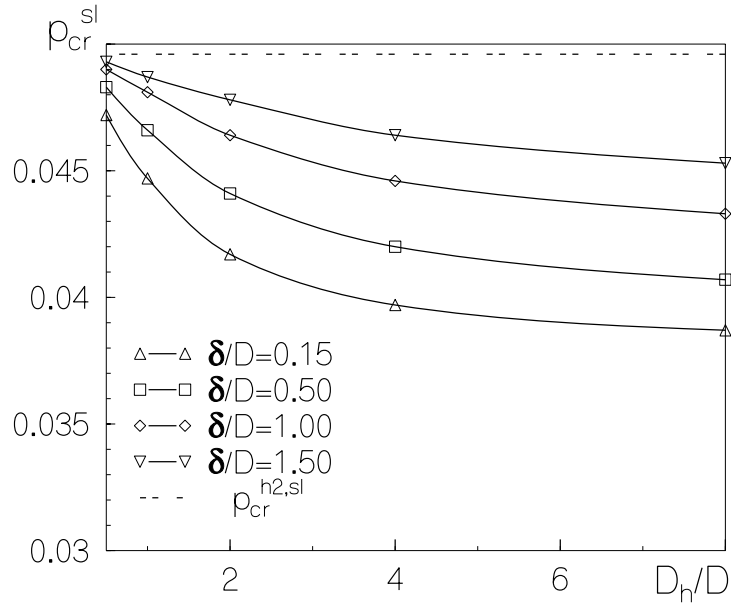


Figure 6: Parameter  $p_{cr}^{sl}$  versus  $D_h/D$  for different values of the dimensionless spacing between the fiber and the hole  $\delta/D$  (the case of a sliding contact between the fiber and the matrix).



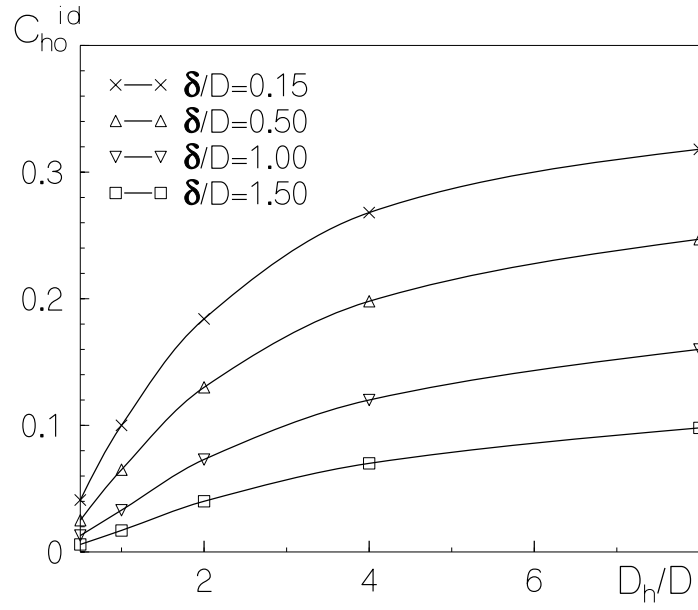


Figure 7: Values of the parameter  $C_{ho}^{id}$  versus the dimensionless diameter of the hole  $D_h/D$  calculated for the case of an ideal fiber-matrix bonding.

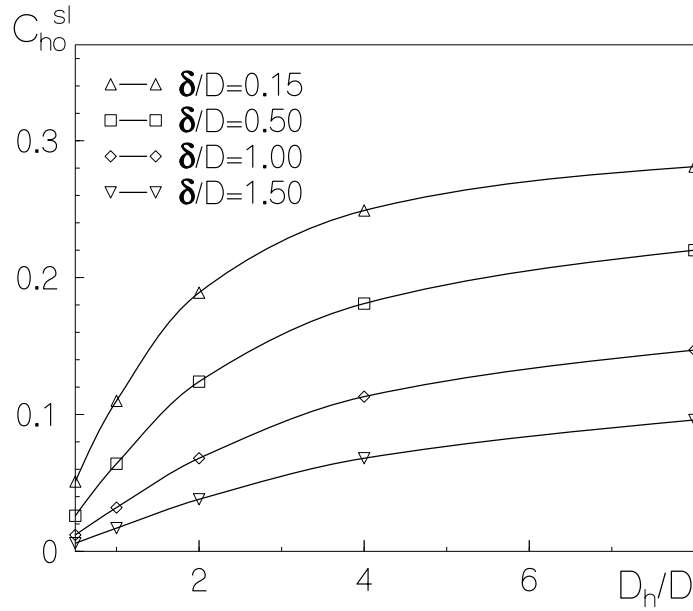


Figure 8: Values of the parameter  $C_{ho}^{sl}$  versus the dimensionless diameter of the hole  $D_h/D$  calculated for the case of a sliding contact between the fiber and the matrix.

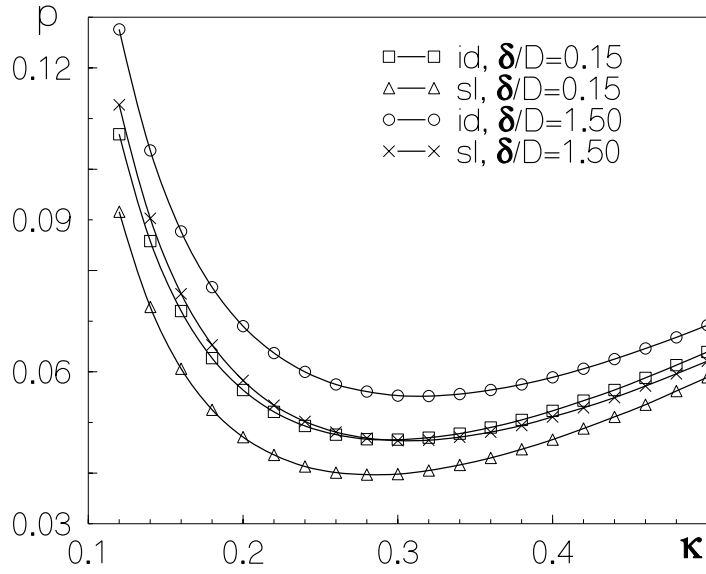


Figure 9: Dependencies of the parameter  $p$  ( $p^{id}$  and  $p^{sl}$ ) on the wave formation parameter  $\kappa$  for some values of  $\delta/D$ , and two different types of interface conditions (a perfect bonding and a sliding contact between the fiber and the matrix).

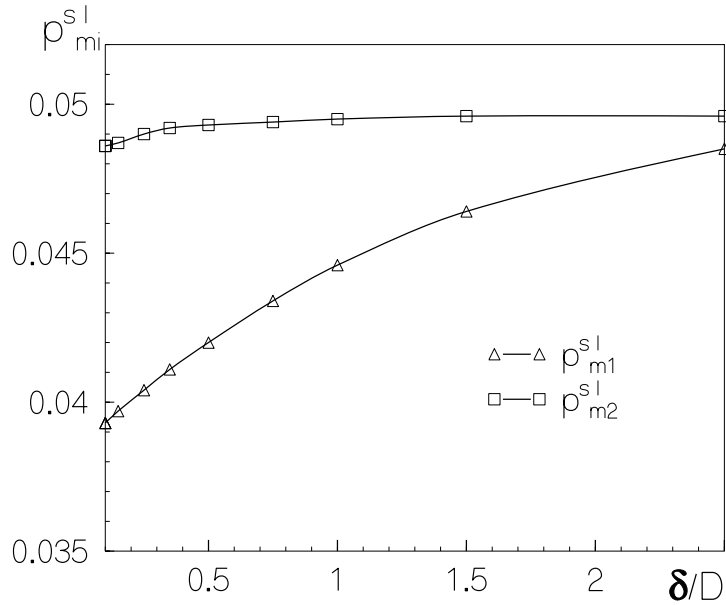


Figure 10: Values of  $p_{mi}^{sl}$  calculated in the presence of a sliding contact between the fiber and the matrix with allowance for the effects of a hole of a diameter  $D_h = 4D$  for the s.l.f.s of the fiber in the matrix of the first type (values  $p_{m1}^{sl}$ ) and of the second type (values  $p_{m2}^{sl}$ ).

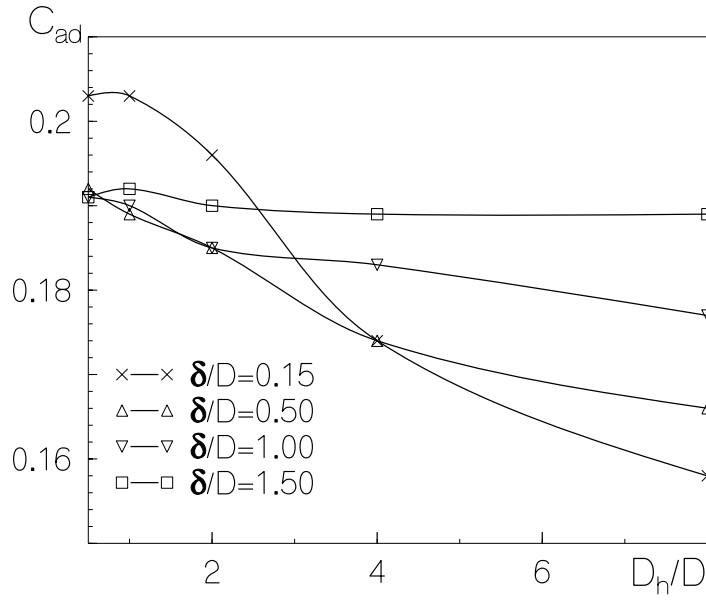


Figure 11: Parameter  $C_{ad}$  versus the dimensionless diameter of the cylindrical hole  $D_h/D$  calculated with different values of the dimensionless spacing between the fiber and the hole  $\delta/D$ .

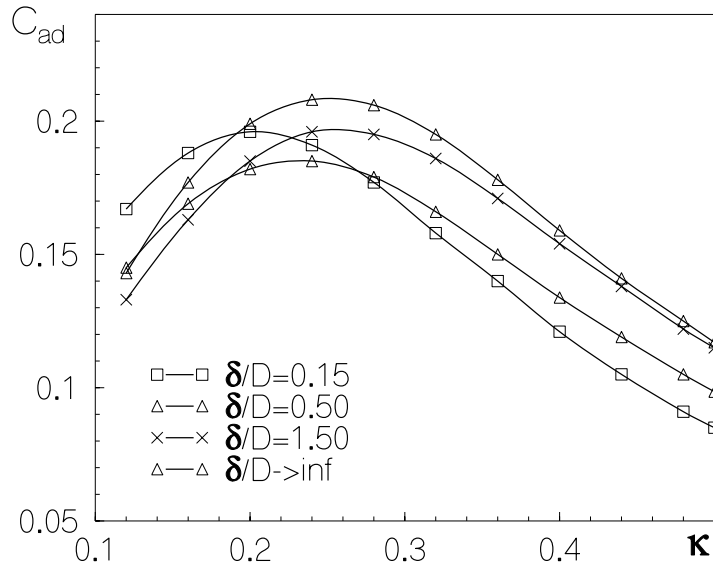


Figure 12: Values of the parameter  $C_{ad}$  as a function of the wave formation parameter  $\kappa$ .

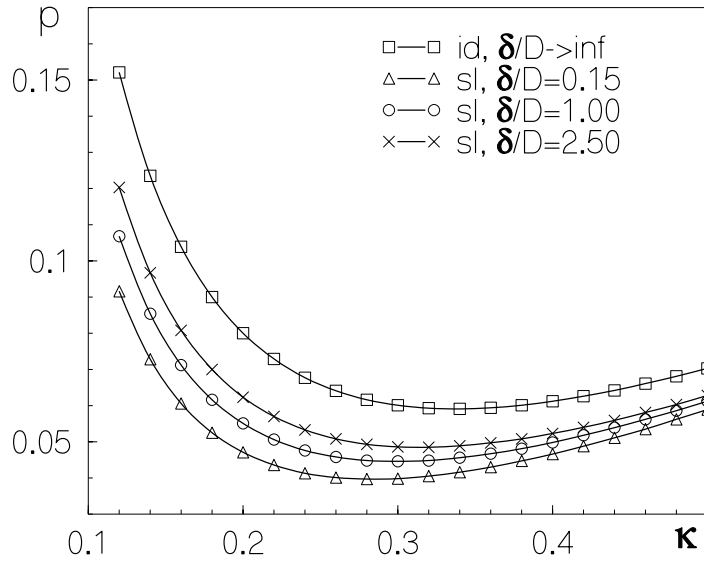


Figure 13: Loading parameter  $p$  versus  $\kappa$  for the 'ideal' case of a fiber in a homogeneous matrix without holes in the presence of a perfect bonding at the fiber-matrix interfaces in comparison with the cases of a fiber in a matrix weakened by a hole in the presence of a sliding contact at the interface.

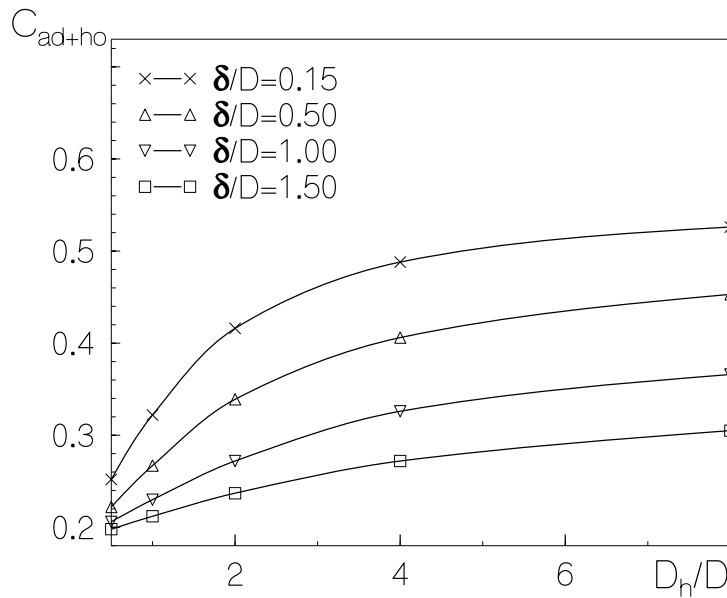


Figure 14: Values  $C_{ad+ho}$  versus the dimensionless diameter of the hole  $D_h/D$ .